

Doubling of coastal erosion under rising sea level by mid-century in Hawaii

Tiffany R. Anderson, Charles H. Fletcher, Matthew M. Barbee, L. Neil Frazer & Bradley M. Romine

Natural Hazards

Journal of the International Society
for the Prevention and Mitigation of
Natural Hazards

ISSN 0921-030X

Nat Hazards
DOI 10.1007/s11069-015-1698-6



Your article is protected by copyright and all rights are held exclusively by Springer Science +Business Media Dordrecht. This e-offprint is for personal use only and shall not be self-archived in electronic repositories. If you wish to self-archive your article, please use the accepted manuscript version for posting on your own website. You may further deposit the accepted manuscript version in any repository, provided it is only made publicly available 12 months after official publication or later and provided acknowledgement is given to the original source of publication and a link is inserted to the published article on Springer's website. The link must be accompanied by the following text: "The final publication is available at link.springer.com".

Doubling of coastal erosion under rising sea level by mid-century in Hawaii

Tiffany R. Anderson¹ · Charles H. Fletcher¹ ·
Matthew M. Barbee¹ · L. Neil Frazer¹ ·
Bradley M. Romine²

Received: 28 January 2015 / Accepted: 11 March 2015
© Springer Science+Business Media Dordrecht 2015

Abstract Chronic erosion in Hawaii causes beach loss, damages homes and infrastructure, and endangers critical habitat. These problems will likely worsen with increased sea level rise (SLR). We forecast future coastal change by combining historical shoreline trends with projected accelerations in SLR (IPCC RCP8.5) using the Davidson-Arnett profile model. The resulting erosion hazard zones are overlain on aerial photos and other GIS layers to provide a tool for identifying assets exposed to future coastal erosion. We estimate rates and distances of shoreline change for ten study sites across the Hawaiian Islands. Excluding one beach (Kailua) historically dominated by accretion, approximately 92 and 96 % of the shorelines studied are projected to retreat by 2050 and 2100, respectively. Most projections (~80 %) range between 1–24 m of landward movement by 2050 (relative to 2005) and 4–60 m by 2100, except at Kailua which is projected to begin receding around 2050. Compared to projections based only on historical extrapolation, those that include accelerated SLR have an average 5.4 ± 0.4 m (\pm standard deviation of the average) of additional shoreline recession by 2050 and 18.7 ± 1.5 m of additional recession by 2100. Due to increasing SLR, the average shoreline recession by 2050 is nearly twice the historical extrapolation, and by 2100 it is nearly 2.5 times the historical extrapolation. Our approach accounts for accretion and long-term sediment processes (based on historical trends) in projecting future shoreline position. However, it does not incorporate potential future changes in nearshore hydrodynamics associated with accelerated SLR.

Electronic supplementary material The online version of this article (doi:[10.1007/s11069-015-1698-6](https://doi.org/10.1007/s11069-015-1698-6)) contains supplementary material, which is available to authorized users.

✉ Tiffany R. Anderson
tranders@hawaii.edu

¹ Department of Geology and Geophysics, School of Ocean and Earth Science and Technology, University of Hawaii at Manoa, 1680 East-West Road, POST Room 721, Honolulu, HI 96822, USA

² University of Hawaii Sea Grant College Program c/o Department of Land and Natural Resources, Office of Conservation and Coastal Lands, 1151 Punchbowl Street, Room 131, Honolulu, HI 96813, USA

Keywords Sea level rise · Erosion · Hawaii · Reef · Shoreline

1 Introduction

Coastal erosion negatively affects Hawaii's tourism-based economy, limits public beach access and cultural practices, and damages homes, infrastructure, and critical habitats for endangered wildlife. Fletcher et al. (2013) found that seventy percent of all sandy shoreline on the islands of Oahu, Maui, and Kauai are chronically eroding; nine percent of these shorelines were completely lost to erosion during their 80-year analysis period. As global mean sea level is predicted to rise dramatically over the next century (Church et al. 2013; Kopp et al. 2014), government officials, nonprofit groups, and property owners wonder how increased sea level rise (SLR) will affect their ongoing struggle to manage retreating shorelines.

Tidal records indicate that the Hawaiian Islands of Maui, Oahu, and Kauai have experienced at least a century of relative SLR at rates from 1.50 to 2.32 mm/y. Romine et al. (2013) investigated shoreline trends on islands with different SLR rates and concluded that SLR is linked to coastal erosion in Hawaii. However, shoreline change rates around each island vary greatly (erosion rates up to -1.8 ± 0.3 m/year and accretion rates up to 1.7 ± 0.6 m/year; Romine and Fletcher 2013), where segments of erosion and accretion were separated by tens to hundreds of meters alongshore despite rather homogeneous island-wide SLR trends. This suggests that the influence of SLR on shoreline change is presently minor compared with sediment availability (sum of sources and sinks) related to human impacts and persistent physical processes such as eolian transport, cross-shore transport, and gradients in longshore sediment transport.

Future accelerated SLR is expected to have an increased effect on coastal morphology (Stive 2004) and to promote erosion of numerous Hawaiian beaches (Romine et al. 2013). The Intergovernmental Panel on Climate Change (IPCC) Fifth Assessment Report (AR5; 2013) projects 0.52–0.98 m of SLR by 2100 relative to 1986–2005 for Representative Concentration Pathway (RCP) 8.5 (the “business as usual” scenario; Church et al. 2013). This gives a rate during 2080–2100 of 8–16 mm/year, up to an order of magnitude larger than the Honolulu tide gauge SLR rate (1.50 ± 0.25 mm/year; <http://tidesandcurrents.noaa.gov>) for the previous century (1905–2006) when the Honolulu SLR trend was similar to the estimated global mean trend (e.g., 1.7 ± 0.2 mm/year; Church and White 2011). The current IPCC projections may underestimate SLR because they do not include the results of recent studies indicating increased ice melt for Greenland (Helm et al. 2014) and West Antarctica (Joughin et al. 2014; Rignot et al. 2014).

Sediment transport, and thus shoreline migration, is the result of multiple nonlinear processes that dynamically interact with existing morphology over a variety of time and spatial scales (Stive et al. 2002; Hanson et al. 2003). As a result of increased SLR, sediment-deficient low-lying coastal areas will experience enhanced erosion and inundation determined by sediment availability and local coastal slope. Beaches will be further shaped by changes in sediment transport patterns as a result of higher water levels over fringing reefs (Grady et al. 2013), climate-related modifications in reef geomorphology and sediment production (Perry et al. 2011), and changes in storminess and wave climate (Aucan et al. 2012).

Numerical models have the potential to describe beach evolution more accurately than long-term trends, but often require data at spatial and temporal densities that are not available. Such methods are therefore difficult to apply to the multidecadal timescales that are the focus of this paper (Hanson et al. 2003). For baseline assessment over large coastal regions, it is therefore necessary to develop empirical methods that provide a first-order approximation of erosion exposure and its uncertainty. Communicating hazard uncertainty to coastal managers (Pilkey et al. 1993; Thieler et al. 2000; Pilkey and Cooper 2004, etc.) enables them to make decisions based on levels of risk. It also helps coastal managers understand that as new data become available, updated projections will replace old ones (Pilkey and Cooper 2004).

Historical data are commonly used to provide long-term information on coastal erosion (Fig. 1), but extrapolating historical trends is insufficient given the projected accelerations in SLR. Hwang (2005) suggests multiplying the historical trend by a SLR adjustment factor, such as 10 %, and then extrapolating the adjusted trend. Although easy to implement, this approach does not allow for acceleration and assumes that the effect of accelerated SLR on coastal erosion is proportional to the historical rate, which is not physically justifiable. Komar et al. (1999), following Gibb (1995), combine the extrapolated long-term trend, a rate of beach retreat due to projected SLR, and dune erosion due to extreme storms to determine a coastal hazard zone (CHZ); however, since the authors found sediment movement within the Oregon Coast study area to be dominated by episodic events, only the dune recession component was used to determine the CHZ. Hawaii beaches, in contrast, are highly influenced by sediment flux due to persistent or seasonal wave conditions.

Pilkey and Cooper (2004) suggest extrapolating historical shoreline trends in combination with an “expert eye” to assess the effects of geologic constraints, sediment availability, and engineered structures on shoreline migration. Yates et al. (2011) combine historical trend extrapolation with the Bruun rule (Bruun 1962), as suggested by the

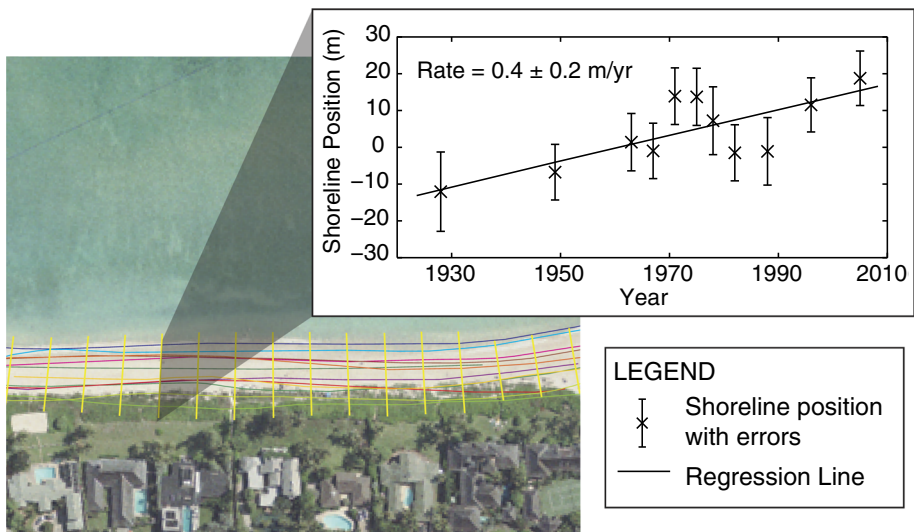


Fig. 1 Relative cross-shore positions are recorded along transects (yellow vertical lines) spaced 20 m apart along the shore. The shoreline change rate is the slope of the line fit to the historical data

EUROSION (2004) project; they also give an example of Pilkey and Cooper's (2004) "expert eye," by averaging trends within a homogeneous region and then combining the extrapolated average with Bruun estimates. Houston and Dean (2014) use sediment budgets to quantify sources of shoreline change in Florida. Like Yates et al. (2011), they use the Bruun model to account for the effects of SLR.

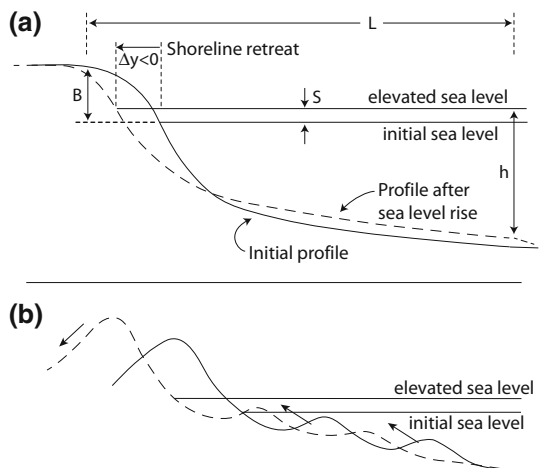
Recently, Ranasinghe et al. (2011) tested their process-based probabilistic coastline recession model on Narrabeen Beach, Australia. Although they used a temporally dense, 30-year collection of wave- and water-level data, the authors speculate that global wave hindcast models (e.g., WAVEWATCH III) would produce similar coastal recession predictions. Gutierrez et al. (2011) produced probabilistic predictions of shoreline retreat under accelerated SLR using a Bayesian network (BN). Their BN identified SLR as the major influence on shoreline stability in their application to the Atlantic coast. Using the same parameters as Gutierrez et al. (2011), Yates and Le Cozannet (2012) identified geomorphology (i.e., rocky cliffs and platforms, erodible cliffs, beaches, and wetlands) as the major influence on shoreline stability, finding that the inclusion of alongshore sediment transport, sediment budget, and anthropogenic activities may improve BN performance on European coasts. For recent reviews of shoreline change prediction incorporating SLR, see Cazenave and Le Cozannet (2013), Fitzgerald et al. (2008), and Shand et al. (2013).

The aforementioned approaches of Komar et al. (1999), Yates et al. (2011), and Houston and Dean (2014) estimate shoreline change by quantifying the separate mechanisms of beach change and assuming their effects are additive. Each approach includes an estimate of shoreline change due to projected SLR. Yates et al. (2011) and Houston and Dean (2014) employ the often-used geometric relation known as the Bruun rule (Bruun 1962, 1988; Schwartz 1967). Based on the conservation of volume, Bruun (1962) proposed that, in the absence of sediment sources and sinks, a beach profile gradually re-equilibrates after a rise in relative mean sea level, as sediment is eroded from the upper beach profile and deposited onto the adjacent seafloor. Bruun's rule (Fig. 2a):

$$\Delta y = -S \times \frac{L}{h + B} = -\frac{S}{\tan \beta} \tag{1}$$

relates shoreline change Δy ($\Delta y < 0$ indicates retreat) to sea level rise S , where L is the horizontal length of the active profile, h is the depth of the active profile base, and B is the

Fig. 2 a According to the Bruun rule, an increase in sea level S causes a shoreline retreat R due to erosion of the upper beach and sediment deposition offshore. **b** In contrast, the R-DA model assumes that all sediment is transported landward while still resulting in an upward and landward translation of the nearshore profile and dune. Arrows indicate the general direction of net sediment movement



berm crest elevation above sea level. Here $\tan \beta$ is the average slope of the active profile (e.g., Komar 1998).

On its own, the Bruun model is virtually unusable in open-ocean coastal environments due to the theory's limiting assumptions of physical setting (constant longshore transport, no sediment sources or sinks) (List et al. 1997; Thieler et al. 2000; Cooper and Pilkey 2004). The assumption of no alongshore change in the sediment budget is an important limitation for Pacific Island beaches where sediment exchange, especially longshore transport, can dominate shoreline morphology (Dail et al. 2000; Norcross et al. 2003b). Although the Bruun rule projects only shoreline recession due to SLR, we find shorelines accreting where sediment gain offsets the landward migration due to SLR. Variations of the Bruun rule have been proposed that include landward transport to dunes (Rosati et al. 2013) and net longshore sediment movement (Hands 1980, 1983; Dean and Maurmeyer 1983; Everts 1985). Similarly, Yates et al. (2011) and Houston and Dean (2014) combine the Bruun rule with estimates of the net sediment budget. The shoreface translation model (Cowell et al. 1995) also assumes that the profile shape remains constant and is translated in response to a rise in relative sea level, based on conservation of volume (like Bruun), net sediment budget, and surrounding geology. Allowing sediment sources to offset the "Bruun effect" (beach profile readjustment in response to SLR) has been found to improve model predictions (SCOR Working Group 89, 1991). However, large uncertainties in sediment budget estimates can diminish their value in improving shoreline forecasts based on the Bruun approach (List et al. 1997).

Even with terms representing the sediment budget, the Bruun model remains controversial. Some field and laboratory experiments support the Bruun model (e.g., Hands 1979, 1980, 1983; Mimura and Nobuoka 1995; Zhang et al. 2004), while others argue that experimental flaws hinder such experiments from validating the model (e.g., SCOR Working Group 89, 1991; Thieler et al. 2000; Cooper and Pilkey 2004; Davidson-Arnott 2005). To date, no study has produced comprehensive, well-accepted verification of the Bruun model (Ranasinghe and Stive 2009.) In reviewing earlier studies, however, the Scientific Committee on Ocean Research (SCOR working Group 89 1991) found that the Bruun model was valid in its upward and landward translation of the profile, but that its quantitative estimates are very coarse approximations.

A geometric model that has emerged as an alternative to the Bruun rule was proposed by Davidson-Arnott (2005). The model, referred to as R-DA, is similar to the Bruun model, in that an upward and landward translation of the profile is predicted, but the underlying assumptions of the two models are quite different. In the R-DA model, it is assumed that as sea level rises, the beach and foredune are eroded and sediment is transported landward, causing a landward and upward migration of the beach–foredune intersection. Similarly, there is a net onshore migration of sediment in the nearshore, causing an upward and landward migration of the shoreline and the seaward limit of the active profile (Fig. 2b). Davidson-Arnott (2005) notes that this landward sediment movement is consistent with observed landward dune migration, and inconsistent with the Bruun assumption that sediment is strictly eroded from the beach and deposited in the nearshore. The expression for shoreline migration given by R-DA is identical in form to that of Bruun, in that landward migration Δy is equal to $(\tan \beta)^{-1}$ times the amount of SLR (right side of Eq. 1), but in R-DA, the term $\tan \beta$ is the nearshore slope averaged over only the submerged portion of the active beach profile, not the entire profile, so it does not depend on B .

By explicitly including beach–dune sediment exchange and landward eolian sediment transport, the R-DA model allows for preservation of the foredune system under rising sea levels. Davidson-Arnott (2005) hypothesizes that increased sea level will cause more

frequent scarping of the foredune, which decreases vegetative covering; because sediment is more frequently exposed, there is an increase in the sediment transported from the face of the dune to the leeward dune slope. He further notes that when nearshore bars are present, they tend to oscillate about an equilibrium depth and distance to shore depending on wave activity. As sea level rises, the oscillating bar position gradually shifts landward as it adjusts to the new equilibrium depth and distance. He argues that this behavior holds for all sediment within the nearshore portion of the profile, providing a sediment source for the landward migrating beach and dune complex. Although the R-DA model, like Bruun, assumes an entirely sand-bottomed profile, the R-DA hypotheses may be a more realistic basis for understanding a Hawaiian fringing reef setting where reef-fringed dune–beach complexes are seen migrating landward across the underlying limestone platform that contours the slope of the shallow nearshore.

We follow Yates et al. (2011), by modeling shoreline change with a combination of historical rates and a SLR-based mechanism, but we use R-DA instead of Bruun. Here, historical rates are used to implicitly include net sediment fluxes. Compared with process-based models, the empirical method provides a computationally efficient way of estimating future coastal erosion hazards over large geographic regions (spanning islands) using existing historical shoreline data and repeated beach surveys. This approach is particularly useful for reef-fringed islands where seasonal wave regimes interact with intricate reef morphology, thus complicating typical methods of estimating decadal patterns of net sediment transport such as associating transport with incoming wave angle or other process-based methods. We develop probabilistic (80 %) erosion hazard zones which are then overlain on geologic and/or development layers in a geographic information system (GIS). Future rates of shoreline change and distances of retreat (or advance) are also calculated. We analyze ten Hawaiian Island beach study sites representing varying conditions of geology, wave climate, and density of coastal development. We pay close attention to sources of uncertainty and the resulting uncertainty in the projected hazard areas.

2 Methods

Shoreline change in Hawaii is directly related to coastal setting, which varies greatly around each island. After introducing regional coastal settings in Hawaii, we describe the data and our procedure for determining exposure to future erosion hazards.

2.1 Regional setting and study sites

The fringing reef assemblage in Hawaii (Fig. 3) is the result of carbonate accretion and erosion over recent glacial cycles (reviewed in Fletcher et al. 2008). The reef occurs as a shallow insular shelf that slopes gently seaward in the depth range of 0–20 m and abruptly drops off to a deeper, partially sand-covered terrace near 30 m depth. Eolianites originating during the last interglacial and the Holocene (Fletcher et al. 2005) are found in the nearshore and coastal plain. Beachrock slabs exist in the intertidal zone of some beaches, as well as in the nearshore. During glacial periods when sea level was lower, paleochannels were carved into the reef shelf sub-perpendicular to shore, and karstification of the exposed limestone created depressions and bathymetric complexity at depths now less than 10 m (Purdy 1974; Grossman and Fletcher 2004; Bochicchio et al. 2009).

Sandy beaches in Hawaii are generally white in color and lack a terrigenous source. They are the product of reef bioerosion and mechanical erosion and direct production of calcareous material by reef organisms such as foraminifera and echinoderms. Sand grains are mainly biogenic carbonate (Moberly and Chamberlain 1964; Harney et al. 2000), with a small contribution from eroded volcanic rock. The most abundant accumulation of sand on typical low-lying Hawaiian coasts lies in coastal plains that accreted during a late Holocene fall in sea level from around 3000 BP to the pre-modern era (Fletcher and Jones 1996; Grossman and Fletcher 1998). Within the nearshore environment, sediment can accumulate in isolated reef-top karst depressions and in paleochannels (Conger 2005; Bochicchio et al. 2009). Radiocarbon dating of beach, reef-top, and coastal plain sands indicates that most beach sand originated in the late middle to late Holocene, with a notable lack of modern sand (Calhoun and Fletcher 1996; Fletcher and Jones 1996; Grossman and Fletcher 1998; Harney et al. 2000). Consequentially, Hawaiian beaches are often the eroded seaward edge of sand-rich coastal plains (refer to Fig. 3b).

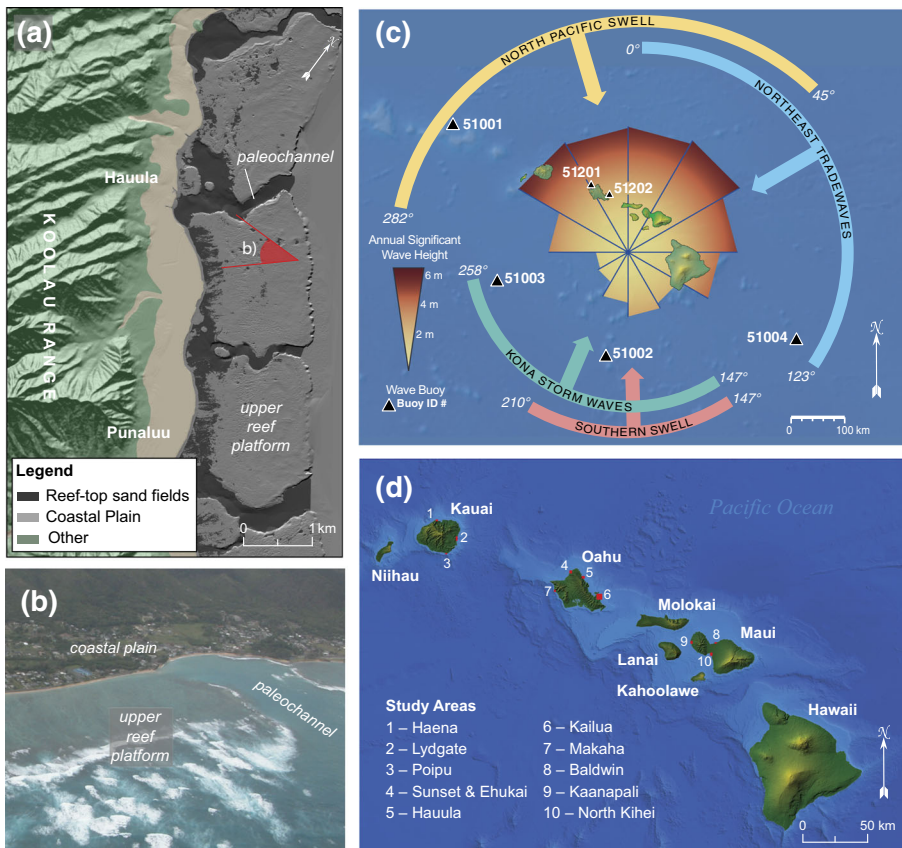


Fig. 3 a–b Fringing reefs dominate coastal geomorphology and are an integral part of sediment dynamics on Hawaii beaches [a modified from Romine et al. (in review); b photo courtesy of the University of Hawaii Coastal Geology Group]. c The dominant swell regimes following Moberly and Chamberlain (1964) are shown with monitoring buoy locations (from Vitousek and Fletcher, 2008). d The ten study locations span three Hawaiian Islands

Wave climate in Hawaii is related to shoreline aspect, with four general wave regimes impacting distinct island regions (Moberly and Chamberlain 1964; Fig. 3). The average directional wave spectrum is dominated by northeast tradewinds and North Pacific swells (Aucan 2006). The persistent tradewinds generate choppy seas with average deepwater wave heights of 2 m from the northeast, during about 75 % of the year (Bodge and Sullivan 1999). North Pacific swells, which peak in the winter, typically generate waves around 4 m while maximum swell events can generate wave heights up to 7.7 m annually (Vitousek and Fletcher 2008). Kona southerly storm waves and southern swell can have episodic impacts on leeward shores. Interannual and decadal cycles such as ENSO and the Pacific Decadal Oscillation contribute to the wave climate variability and thus to episodic coastal erosion (Rooney and Fletcher 2005). Because the wave regimes are directional, beach morphology is dependent on shoreline aspect (Moberly and Chamberlain 1964). Beaches on north- and west-facing shorelines tend to be the longest and widest, with reefs that are narrower, deeper, and more irregular. These north- and west-facing beaches exhibit large seasonal fluctuations due to oblique approaches of seasonally alternating swell directions.

Our ten study areas were selected throughout the Hawaiian Islands of Kauai, Oahu, and Maui (Fig. 3) based on diversity of shoreline aspect, nearshore morphology, and density of development. The characteristics of each site are given in the online supplemental resource (Table S1).

2.2 Projected sea level rise

We use the IPCC AR5 high-end representative concentration pathway (RCP) 8.5 scenario—the “business as usual” scenario (Church et al. 2013). This scenario was selected after discussions with local government agency staff in Hawaii who, like others (e.g., Katsman et al. 2011), prefer the most cautious predictions for long-range planning purposes.

We make the simplifying assumption that predicted sea level is normally distributed and is centered about the IPCC projected median with variance defined as the square of the average distance from the IPCC median estimate to the upper and lower limit of the “likely” range projections (Church et al. 2013).

2.3 Vertical land motion and local SLR

Moore (1970) and others attribute variations in relative SLR rates along the Hawaii Archipelago to variations in lithospheric flexure with distance from Hawaii Island. Because the century-long Honolulu Harbor tide gauge record indicates that sea level has risen at a rate similar to global mean sea level estimates, Moore (1970) and others conclude that the island of Oahu is vertically stable and is located on the lithospheric rise. Caccamise et al. (2005) suggest that variations in upper ocean water masses also contribute to the SLR rate difference between Honolulu and Hawaii Island; however, the authors mention that their current findings cannot be extended to multidecadal timescales due to the limited length (6 years) of their data. Thus, we follow Moore (1970) and assume that the island of Oahu is vertically stable; the Honolulu record then gives *absolute* SLR. We use the linear trend of the Honolulu record as a proxy for absolute SLR of waters surrounding Oahu, Maui, and Kauai. Acceleration of local SLR has not been detected in Hawaii tide gauge records, over the century of record, likely because its signal has been masked by variability in climate (e.g., tradewinds; Merrifield and Maltrud 2011).

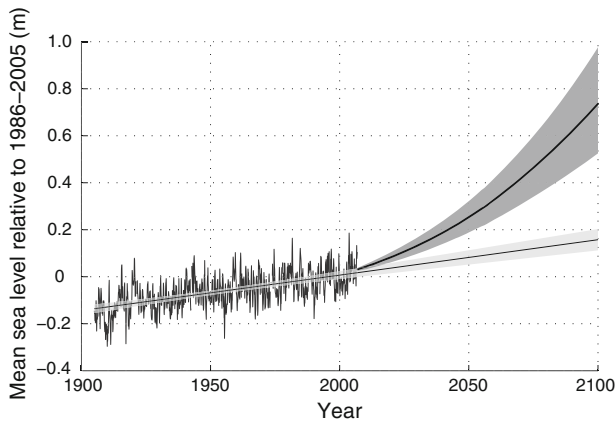


Fig. 4 Monthly mean sea level at Honolulu Harbor between 1905 and 2006 is shown with the trend (*thin black line*) and 95 % confidence band (*light gray band*), and the IPCC AR5 RCP 8.5 sea level projection median (*thick black line*) and “likely” range (*dark gray band*)

Our approach (explained in detail in Sect. 2.6) involves extrapolating the historical shoreline change trend, which inherently includes the effects of historical rates of *relative* SLR, including island subsidence. We assume that vertical land velocity was constant during the historical period; hence, SLR *in excess* of the historical trend is the IPCC AR5 projected global mean sea level estimate (*absolute* future sea level projection) minus the linearly extrapolated Honolulu tide gauge trend (proxy for *absolute* historical sea level in Hawaii; Fig. 4). This excess SLR is the same for each island. The Honolulu SLR trend is 1.50 ± 0.25 mm/year for the period 1905–2006 (<http://tidesandcurrents.noaa.gov>), which spans the period of historical shoreline data in the study areas. The variance of the excess SLR is the sum of the variances of the IPCC projection and the Honolulu tide gauge projection.

2.4 Beach profiles

The US Geological Survey (USGS), in coordination with the University of Hawaii, conducted biannual surveys of cross-shore beach profiles during a 5-year study (1994–1999) of beaches on the islands of Oahu and Maui (Gibbs et al. 2001). University researchers have extended this survey to include biannual beach profiles over the period 2006–2008 at 35 locations in Oahu and at 27 locations in Kauai.¹ During each survey, specific morphologic features along the profile were recorded such as the berm crest, high water, and the beach toe. The beach toe (Bauer and Allen 1995) is the base of the foreshore and is commonly used to demark the shoreline location on Hawaii beaches (e.g., Fletcher et al. 2003; Norcross et al. 2003a).

The profiles at some locations do not extend seaward past what is typically defined as the depth of closure (DoC) (e.g., Hallermeier 1981) because of the presence of shallow fringing reefs. Here we follow Cowell and Kench (2000) who suggest that the intersection

¹ Cross-shore elevations of the beach were collected by University of Hawaii researchers using the same methods described in Gibbs et al. (2001). The University of Hawaii Coastal Geology Group provided the raw data.

of the sandy profile with the reef platform is effectively the seaward extent of the active profile and is thus the DoC on reef-bottomed profiles. For a sandy bottom, the seaward extent of the active profile is taken to be the point at which the profiles from biannual surveys converge.

The nearshore slope of the active profile, defined here as the slope between the seaward extent of the active profile and the beach toe, is estimated at each alongshore location. Histograms of the slopes (one histogram for each alongshore location) suggest that slopes are normally distributed. When more than one profile location is present within a study area, cubic splines are used for interpolation. Summary data for the profiles are provided in Table S2 of the online supplemental resource.

2.5 Historical shoreline change

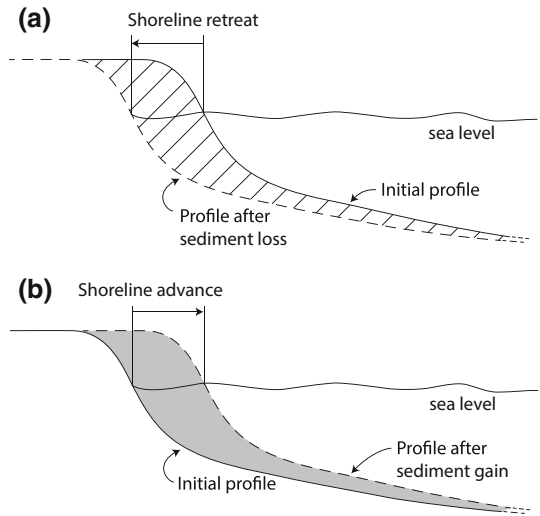
Shoreline positions were extracted from high-resolution aerial photographs and NOAA topographic charts (T-sheets) by University of Hawaii researchers as part of the USGS National Assessment of Shoreline Change (Fletcher et al. 2013). Approximately shore-normal transects were cast 20 m apart in the alongshore direction, and the relative cross-shore distance from each shoreline to the offshore baseline was measured, creating a time series of shoreline positions at each alongshore location (refer to Fig. 1). Five to eleven historical shorelines were used in each of the study areas from 1900 to 2008. The Baldwin study area on the Island of Maui used the least number of historical shorelines (five) because the data prior to 1975 were dropped to exclude the effects of sand mining that occurred up until the early 1970s. Temporal and spatial data extents for each study area, along with ranges of data uncertainty, are provided in the online supplemental resource (Table S3).

The equation $y(t) = b + r(t - \bar{t})$ is fit to the N historical shoreline data points at each transect using weighted least squares (WLS) regression (e.g., Douglas and Crowell 2000). Here, b is the intercept, r is the rate (positive indicates accretion), and \bar{t} is the mean of historical survey times which is used to condition matrices in regression procedures. To reduce large fluctuations in rates among adjacent transects, rates are smoothed in the alongshore direction using a running [1 3 5 3 1] average. The survey errors used in the WLS procedure (see Table S3, online resource) are calculated by the method in Romine et al. (2013) from seven types of data error. In order to be robust to data outliers, the extrapolated shoreline positions are given a generalized Student's t distribution (e.g., Davison 2003, p. 140) with $N - 2$ degrees of freedom, and the least-squares mean and standard deviation are used for the location and scale parameters, respectively.

2.6 Determining future hazard areas

To apply a simple model to a complex system, it is necessary to make some simplifying assumptions. We assume that there exists an equilibrium profile shape under constant forcing conditions (e.g., Fenneman 1902; Bruun 1962; Dean 1991). Storm and seasonal swells perturb the profile shape, while subsequent persistent wave conditions and sediment supply steer it back toward its median sea state equilibrium. Hence, in the absence of any change in relative sea level, the beach profile can be thought to migrate seaward (or landward) when sediment is added (or lost) (Fig. 5) over multi-year to decadal timescales. In fringing reef environments, Muñoz-Pérez et al. (1999) used over 50 profiles from seven beaches to confirm that reef-fronted beaches can have an equilibrium shape; however, they caution there is theoretically no equilibrium profile within a distance of about 10–30 times

Fig. 5 **a** Sediment loss in the absence of any sea level change causes the shoreline to retreat. Conversely, **b** sediment gain causes the shoreline to advance seaward



the depth at the reef edge. Since there are currently no observational studies validating this principle, and Hawaiian beaches typically exceed this distance, we assume that profiles can reach equilibrium on beaches not satisfying this condition.

In the presence of strictly sea level rise (no sediment gain/loss), equilibrium profile theory assumes that beaches keep their general shape, while readjusting to persistent wave conditions at elevated sea levels (Bruun 1962). The presence of a fringing reef challenges this assumption because heightened water level over the reef changes the amount of wave energy that impacts the beach. Although recent studies have made progress in understanding hydrodynamic flow over fringing reefs under potential climate-induced changes in storminess and sea level (e.g., Péquignet et al. 2014), these processes remain poorly understood. Thus, we make the simplifying assumption that the profile shape of reef-protected beaches remains constant as sea level rises.

Our treatment here is similar to that of Yates et al. (2011) with differences that will be noted below. Shoreline change Δy_{total} (negative change indicates retreat) is the sum of the change due to net sediment availability, Δy_{sed} , and the change due to profile readjustment after a rise in relative mean sea level, Δy_{SL} . Here, sediment availability includes all sources and sinks: cross-shore mechanisms (e.g., eolian transport, sediment lost/gained from the seaward edge of the active profile), and sediment changes due to spatial variations in alongshore transport, reef sediment production, dredging, nourishment, etc.

It is helpful to regard the sea level adjustment Δy_{SL} as the sum of (1) Δy_{SL_hist} , the portion of the extrapolated historical change due to historical SLR, and (2) Δy_{SL_ex} , the change in response to excess SLR, i.e., SLR that *exceeds* the extrapolated historical trend of SLR (Fig. 6a). Similarly, the term Δy_{sed} can be expressed as the sum of (1) Δy_{sed_hist} , the extrapolated historical change due to sediment availability, (2) Δy_{sed_SL} , the change due to sediment availability caused by excess SLR, and (3) Δy_{sed_CC} , the change due to non-SLR influences on the sediment budget; these include all processes that may change with future climate change such as wave climate, storm frequency and amplitude, and ENSO patterns.

The total change, Δy_{total} , is thus the sum of five terms: Δy_{SL_hist} , Δy_{SL_ex} , Δy_{sed_hist} , Δy_{sed_SL} , and Δy_{sed_CC} in which the pair $\Delta y_{sed_hist} + \Delta y_{SL_hist}$ comprises historical change, Δy_{hist} . With this replacement, the total change at any given alongshore location becomes

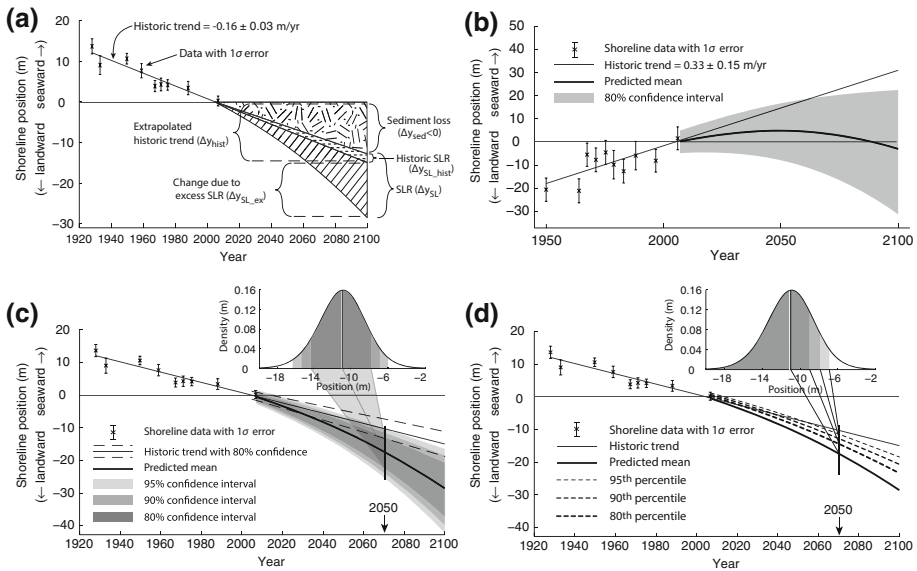


Fig. 6 **a** In the schematic, increased SLR (in excess of historical trends) contributes to increased shoreline recession on an eroding beach. The ratio of sea level induced shoreline change to overall change increases from 2005 to 2100 due to varying acceleration in the sea level curve over time. Historical shoreline data (exes with *error bars*) from one transect in the historically accreting Kailua **b** study area and one transect in the historically eroding Hauula (**c**, **d**) area are plotted against time, along with the extrapolated historical trend (no future increase in SLR; *thin solid line*), and probable estimates of future shoreline position (with future increase in SLR; *thick solid line* and *shaded regions*). In (**b**), the historically accreting beach is expected to begin retreating by 2050 due to increased SLR. The estimated pdf of shoreline position for year 2050 is shown as an inset in (**c**) and (**d**), with two-tailed confidence intervals in (**c**) and on-tailed confidence intervals in (**d**); each can be used to define erosion hazard areas depending on the planning objective. In (**d**), for example, there is a 95 % probability that the shoreline will be below the *light dashed line* in any given year

$$\Delta y_{\text{total}} = \Delta y_{\text{hist}} + \Delta y_{\text{SL}_{\text{ex}}} + \Delta y_{\text{sed}_{\text{SL}}} + \Delta y_{\text{sed}_{\text{CC}}} \tag{2}$$

Substituting $\Delta y_{\text{total}} = y(t_f) - y(t_0)$ then gives shoreline location at future time t_f as

$$y(t_f) = y(t_0) + \Delta y_{\text{hist}} + \Delta y_{\text{SL}_{\text{ex}}} + \Delta y_{\text{sed}_{\text{SL}}} + \Delta y_{\text{sed}_{\text{CC}}} \tag{3}$$

in which t_0 is a time origin chosen for convenience. In this study, we use \bar{t} , the mean of historical survey times, as the time origin.

If we assume that historical shoreline change follows a linear trend, and profile readjustment, $\Delta y_{\text{SL}_{\text{ex}}}$, follows the geometric adjustment outlined in Davidson-Arnott (2005) [in other words that $\Delta y_{\text{SL}_{\text{ex}}}$ is given by the right-hand side of Eq. 1], then Eq. (3) becomes

$$y(t_f) = y(t_0) + r(t_f - t_0) - \frac{[S(t_f) - S_{\text{hist}}(t_f)]}{\tan \beta} + \Delta y_{\text{sed}_{\text{SL}}} + \Delta y_{\text{sed}_{\text{CC}}} \tag{4}$$

The first two terms, $y(t_0) + r(t_f - t_0)$, are determined from the historical shoreline change model described in Sect. 2.5, and the average nearshore slope, $\tan \beta$, is estimated from profile surveys (Sect. 2.4). The difference $S(t_f) - S_{\text{hist}}(t_f)$ is the difference between predicted sea level and extrapolated historical sea level at future time t_f , as described in

Sect. 2.3. The last two terms, $\Delta y_{\text{sed_SL}}$ and $\Delta y_{\text{sed_CC}}$, are neglected in this study on the assumption that SLR will not significantly alter the sediment budget and that changes in wave climate and storm frequency will not affect it either; recent studies suggest that there will be no significant changes in the twenty-first-century North Pacific wave climate (Hemer et al. 2013; Wang et al. 2014). We include these terms as placeholders mainly to raise awareness that these other influences exist and warrant attention. Absent the last two terms, Equation 4 is similar to Equation 2 in Yates et al. (2011), except that here the R-DA model is being used instead of the Bruun model, and all sediment is assumed to have a large enough grain size to remain within the active profile ($P = 1$).

Our treatment of uncertainty also differs from Yates et al. (2011). A probability density function (pdf) of the total projected shoreline position, $y(t_f)$, is estimated from the pdfs of each contributing unit (Fig. 7). Individual pdfs are first created for (1) the extrapolated historical shoreline position, $y(t_0) + r(t_f - t_0)$, (2) the difference in the projected and current sea levels, $S_f - S_{\text{hist}}$, and (3) the average profile slope, $\tan\beta$. Combining the pdfs in Eq. (4) is performed numerically; the quotient pdf is calculated using Equation 3.2 in Curtiss (1941) and then convolved with the pdf of the historical extrapolation to produce the final pdf of $y(t_f)$. From this final pdf, we obtain the mean and median values, as well as the quantiles $y_\epsilon = F^{-1}(\epsilon)$, where F is the cumulative distribution function of the pdf for the projected shoreline. For example, Fig. 6b shows the contours of the mean, and $y_{0.1}$ and $y_{0.9}$ quantiles (80 % confidence interval) of the projected shoreline change for each year between 2005 and 2100 at one historically accreting alongshore location (positive indicates advance); in this example, a retreat is projected by mid-century. Figure 6c shows the historical extrapolation, the modeled mean, and the 80, 90, and 95 % confidence intervals at one historically retreating alongshore location. For the same location as in Fig. 6c, d depicts $y_{0.8}$, $y_{0.9}$, and $y_{0.95}$, the positions at which, with 80, 90, and 95 % probabilities, respectively, the future shoreline will be landward of the contour line. Figure 8 shows the results for multiple alongshore locations (20 m spaced transects) at specific times; the left column shows net shoreline position change relative to 2005 (negative indicates landward migration), for the years 2050 (black line) and 2100 (gray line), while the right column shows shoreline change rates for the historical time period (dashed line), 2050 (black solid line), and 2100 (gray solid line).

The probability-based approach facilitates financial risk assessments needed for near shore conservation or development. For example, in an area with a 70 % probability of erosion in 50 years, it is sensible to permit construction of a fence but not a residence. It is possible that shoreline managers will prefer erosion hazard zones based on a single level of confidence (e.g., 95 % confidence interval) at a future time, overlaid on geographic layers (property TMKs, aerial photos, special management areas, etc).

3 Results

The mean, and 80 % confidence (bounded by $y_{0.1}$ and $y_{0.9}$) for projected net shoreline change are determined at each transect for the years 2050 and 2100, relative to 2005 (e.g., Fig. 8, left column). As mean and median values are similar (pdfs are only slightly skewed), we report only the mean, using it as an indicator of the amplitude of projected change. Based on time series of projected shorelines, shoreline change rates at study areas (Fig. 8, right column) were calculated for the years 2005 (historical), 2050, and 2100. It can be seen that projected net shoreline change and change rates varied spatially within all

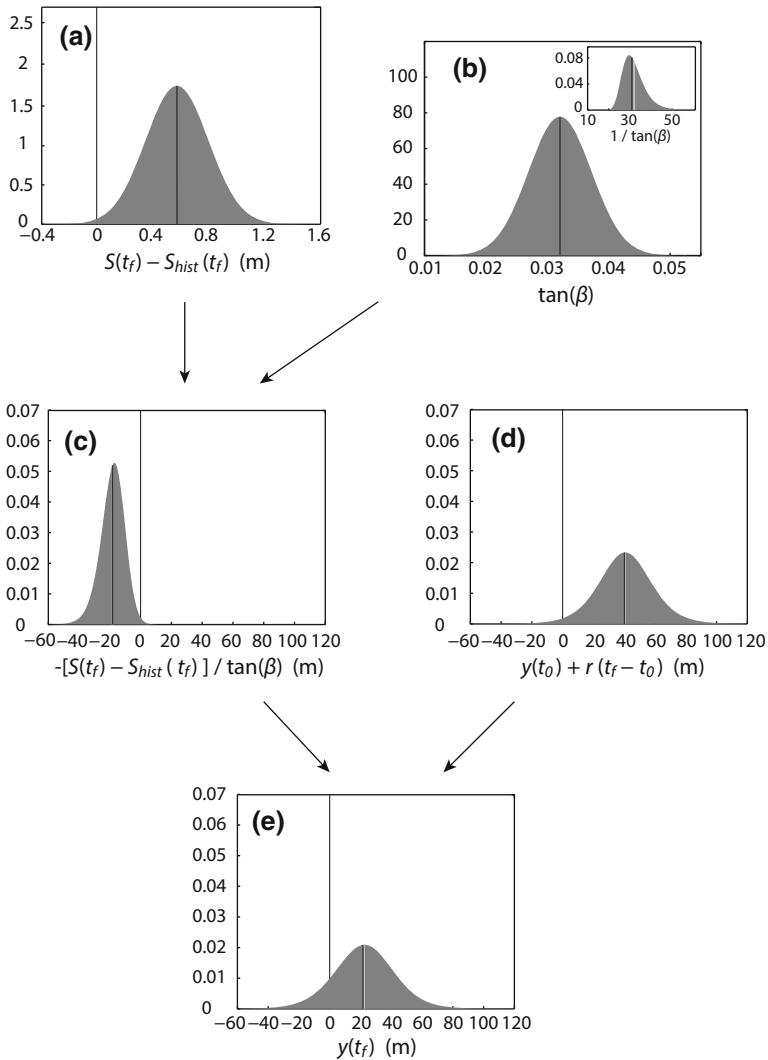


Fig. 7 For the year 2100 ($t_f = 2100$), the pdfs for **a** the difference in the projected and extrapolated historical sea levels, **b** the average profile slope, and **d** the extrapolated historical shoreline position relative to 2005 are combined to produce the **e** pdf for the total projected shoreline relative to 2005 at one transect location. In this example, projected accretion following historical trends **d** is buffered by the landward retreat component in response to increased SLR **(c)**. The mean is depicted by the *dark vertical line*, and the median is the *light line* (may not be visible when the median is nearly identical to the mean)

study areas. As expected, in areas where sediment gain overpowers any profile readjustment due to SLR, such as in Kailua and portions of Kaanapali, shoreline accretion continues, though at a reduced rate.

Figure 9 shows areas exposed to erosion hazards (defined as the 80 % confidence interval) for the years 2050 (yellow) and 2100 (red) at Kaanapali, Maui, projected back into map coordinates and displayed atop a vertical aerial photograph. Mapped hazard areas

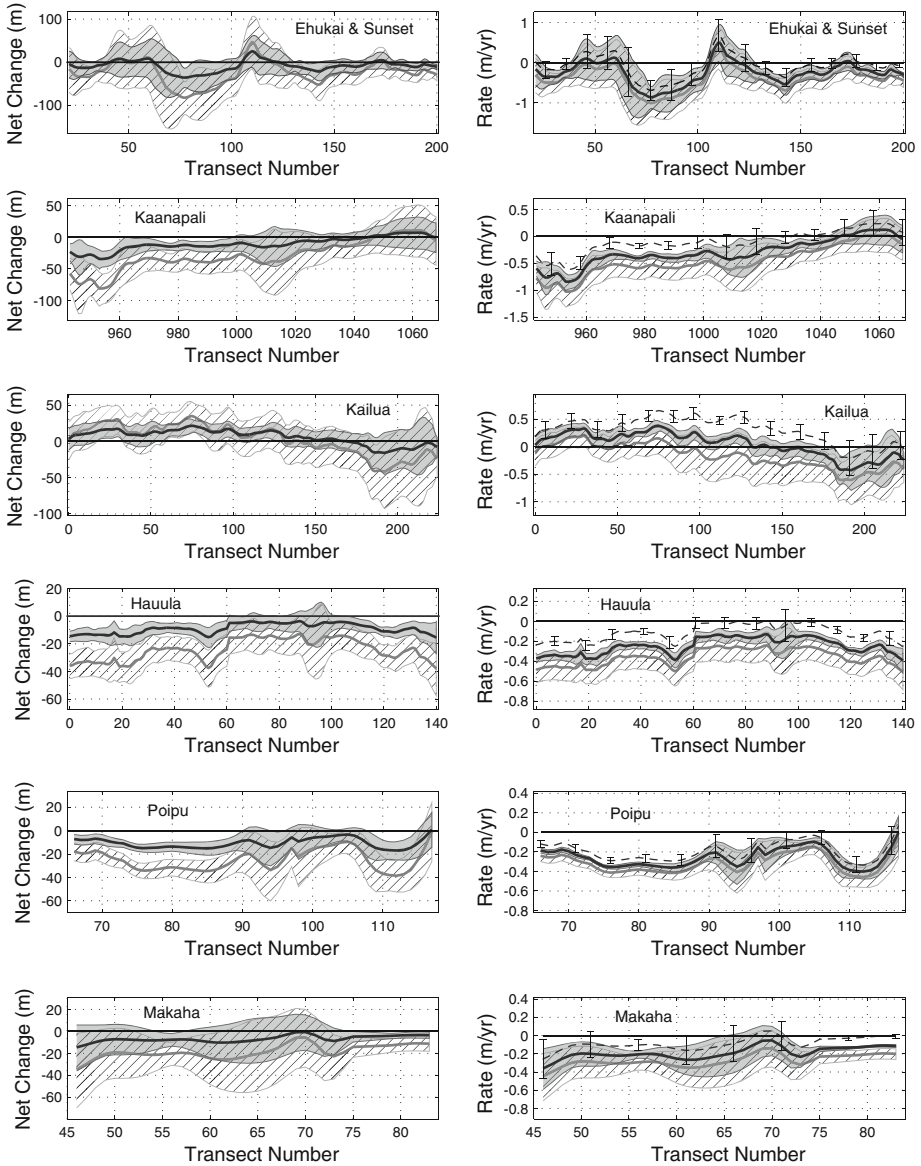


Fig. 8 Left column shoreline change (positive for accretion) relative to 2005 is shown with 80 % confidence band at select locations for 2050 (dark solid line with gray-filled band) and 2100 (gray solid line with diagonal striped band). Right column change rates, shown with 80 % confidence bands, illustrate similar behavior along each shore for the historical time period (dashed line with whiskers), the 2050 projection (dark solid line with gray-filled band), and the 2100 projection (gray solid line with diagonal striped band). Transects are spaced 20 m apart

are truncated by the current shoreline location at their seaward extent for improved usability. Uncertainty values are large, as expected, providing only a broad assessment of potential erosion hazard.

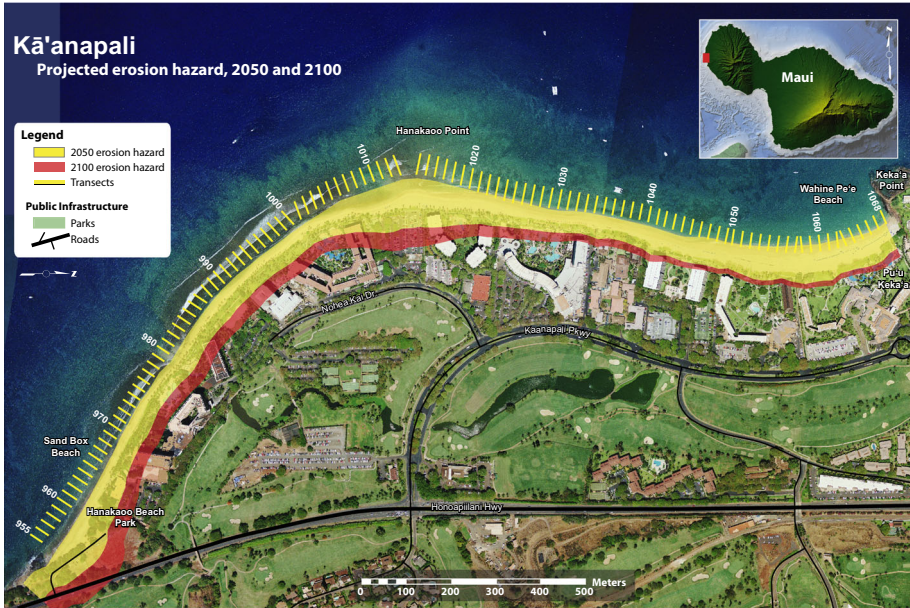
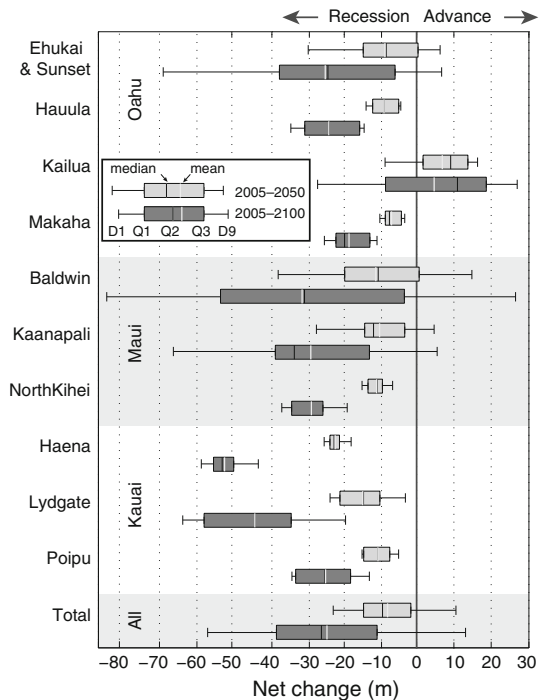


Fig. 9 Example of an erosion hazard area (80 % confidence interval) is shown overlain on an aerial photograph, with a layer displaying public infrastructure (e.g., roads, parks)

Fig. 10 Box and whisker plots show the distribution of net shoreline change for the time periods 2005–2050 (light boxes) and 2005–2100 (dark boxes) at each study site. Box widths indicate the first and third quartiles, i.e., 50 % of the transects within a study area reside within the box limits. Vertical lines show the mean (light-colored line) and median (black line) of net change estimates. Whiskers indicate the first and tenth deciles, containing 80 % of transects. Net shoreline recession between 2005 and 2050 is the dominant trend at all study sites, except for Kailua. Shoreline projections indicate that recession will continue through 2100



The distributions of projected shoreline migration amplitude (one amplitude at each transect) within each study site (Fig. 10) indicate that shoreline recession dominates the 2050 and 2100 projections in all study areas except Kailua. Kailua shows an average seaward migration of 7.1 ± 3.2 m by 2050 that declines to 4.9 ± 6.8 m by 2100. The Ehukai and Sunet, Baldwin, and Kaanapali locations show the most dispersion in migration, as alternating cells of retreat and accretion exist within each study area. Shoreline change rates also indicate dominant retreat historically (Fig. 11), except for Kailua.

The alongshore averages—the mean of all individual means—of projected net shoreline migration and shoreline change rates for each study area are given in Tables 1 and 2, respectively, along with the percent of transects that indicate retreat (negative change rate; Table 2). Because of the small spacing between transects (20 m), we follow Hapke et al. (2010) and Romine et al. (2013), by using the effective number of independent observations (Bayley and Hammersley 1946, Eq. 1) to adjust for correlated data in the computation of the alongshore means. The average net change and average rate over all transects in the ten study sites indicate less severe retreat compared to individual study areas except Kailua. However, these averages are not likely indicative of Hawaii beaches in general because the anomalous accretion in the Kailua area, which comprises roughly 20 percent of combined study area transects, heavily influences the overall averages. To reduce this bias, combined averages excluding the Kailua area are given in Tables 1 and 2.

For comparison, Table 1 includes alongshore averages and the range of net change based on: (1) historical extrapolation only, (2) additional SLR only, and (3) the total

Fig. 11 Shoreline change rates become more recessional over time as a result of modeled recession in response to increased rates of SLR. Shoreline advance at most Kailua transects reverses to recession by 2100

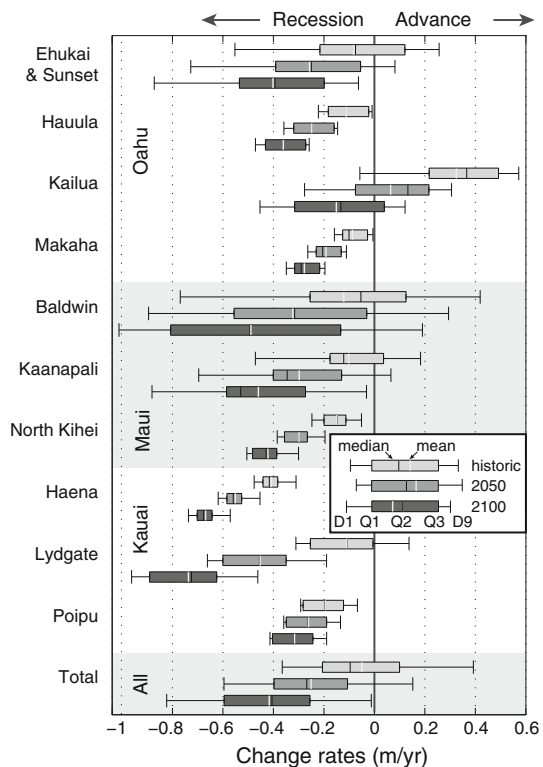


Table 1 Mean projected net shoreline change (\pm std) and range of net change for each study area are shown based on historical extrapolation only, additional SLR only, and the total net change

Island	Region	Timespan	Historical extrapolation only		Additional SLR only		Historical + additional SLR	
			Average net change (\pm std) (m)	Range of net change (m)	Average net change (\pm std) (m)	Range of net change ^a (m)	Average net change (\pm std) (m)	Range of net change (m)
Oahu	Ehukai and Sunset	2005–2050	-3.7 \pm 5.1	-30.9 to 30.4	-5.0 \pm 1.7	-5.0 to -5.0	-8.7 \pm 6.2	-35.9 to 25.3
		2005–2100	-7.8 \pm 8.4	-65.2 to 64.1	-17.4 \pm 5.8	-17.4 to -17.4	-25.2 \pm 10.4	-82.6 to 46.7
	Hauula	2005–2050	-5.0 \pm 0.4	-11.5 to 0.3	-3.9 \pm 1.4	-3.9 to -3.9	-9.0 \pm 0.5	-15.5 to -3.6
		2005–2100	-10.6 \pm 0.6	-24.4 to 0.7	-13.6 \pm 4.7	-13.6 to -13.6	-24.2 \pm 1.0	-38.0 to -12.9
		2005–2050	14.6 \pm 2.5	-9.6 to 29.6	-7.5 \pm 1.0	-10.8 to -4.7	7.1 \pm 3.2	-15.8 to 21.9
Maui	Makaha	2005–2100	30.8 \pm 4.2	-20.3 to 62.4	-25.9 \pm 3.3	-37.4 to -16.1	4.9 \pm 6.8	-41.7 to 34.9
		2005–2050	-3.9 \pm 2.0	-11.6 to 2.3	-3.0 \pm 1.0	-3.0 to -3.0	-6.9 \pm 2.4	-14.6 to -0.7
	Baldwin	2005–2100	-8.3 \pm 3.3	-24.4 to 4.8	-10.4 \pm 3.4	-10.4 to -10.4	-18.6 \pm 3.9	-34.8 to -5.6
		2005–2050	-5.5 \pm 1.5	-83.9 to 36.4	-5.8 \pm 1.0	-9.1 to -3.6	-11.2 \pm 1.9	-87.5 to 32.8
		2005–2100	-11.6 \pm 2.9	-177.2 to 76.8	-20.1 \pm 3.2	-31.4 to -12.5	-31.6 \pm 3.2	-189.6 to 64.4
Kauai	Kaanapali	2005–2050	-4.6 \pm 2.1	-27.7 to 10.9	-5.7 \pm 1.0	-6.5 to -3.4	-10.2 \pm 2.3	-34.2 to 7.5
		2005–2100	-9.6 \pm 3.5	-58.5 to 22.9	-19.6 \pm 3.4	-22.4 to -11.7	-29.2 \pm 3.6	-80.9 to 11.3
	North Kihai	2005–2050	-6.7 \pm 2.2	-12.5 to -0.6	-4.3 \pm 0.8	-4.9 to -3.6	-11.0 \pm 3.2	-16.4 to -4.2
		2005–2100	-14.2 \pm 3.7	-26.3 to -1.3	-14.9 \pm 2.7	-17.0 to -12.5	-29.0 \pm 5.6	-39.9 to -13.8
		2005–2050	-18.4 \pm 5.3	-25.8 to -11.5	-4.1 \pm 1.4	-4.1 to -4.1	-22.5 \pm 1.3	-29.9 to -15.6
Poipu	Lydgate	2005–2100	-38.8 \pm 8.7	-54.5 to -24.3	-14.2 \pm 4.7	-14.2 to -14.2	-53.0 \pm 2.3	-68.7 to -38.5
		2005–2050	-5.0 \pm 1.1	-18.2 to 11.7	-9.9 \pm 2.1	-10.5 to -8.9	-14.8 \pm 1.4	-28.7 to 2.0
	Poipu	2005–2100	-10.5 \pm 1.8	-38.4 to 24.6	-34.2 \pm 7.1	-36.3 to -30.7	-44.6 \pm 2.8	-74.7 to -8.8
		2005–2050	-8.8 \pm 1.4	-15.1 to 2.9	-1.9 \pm 0.7	-1.9 to -1.9	-10.7 \pm 2.0	-17.0 to 1.0
		2005–2100	-18.5 \pm 2.4	-31.9 to 6.1	-6.6 \pm 2.5	-6.6 to -6.6	-25.7 \pm 1.1	-38.5 to -0.5

Table 1 continued

Island Region	Timespan	Historical extrapolation only		Additional SLR only		Historical + additional SLR	
		Average net change (\pm std) (m)	Range of net change (m)	Average net change (\pm std) (m)	Range of net change ^a (m)	Average net change (\pm std) (m)	Range of net change (m)
All Total	2005–2050	-2.2 \pm 0.6	-83.9 to 36.4	-5.8 \pm 0.4	-10.8 to -1.9	-8.0 \pm 0.6	-87.5 to 32.8
	2005–2100	-4.7 \pm 0.9	-177.2 to 76.8	-20.0 \pm 1.3	-37.4 to -6.6	-24.7 \pm 1.1	-189.6 to 64.4
Total (excluding Kaitiua)	2005–2050	-5.9 \pm 0.6	-83.9 to 36.4	-5.4 \pm 0.4	-10.5 to -1.9	-11.3 \pm 0.6	-87.5 to 32.8
	2005–2100	-12.5 \pm 1.0	-177.2 to 76.8	-18.7 \pm 1.5	-36.3 to -6.6	-31.2 \pm 1.1	-189.6 to 64.4

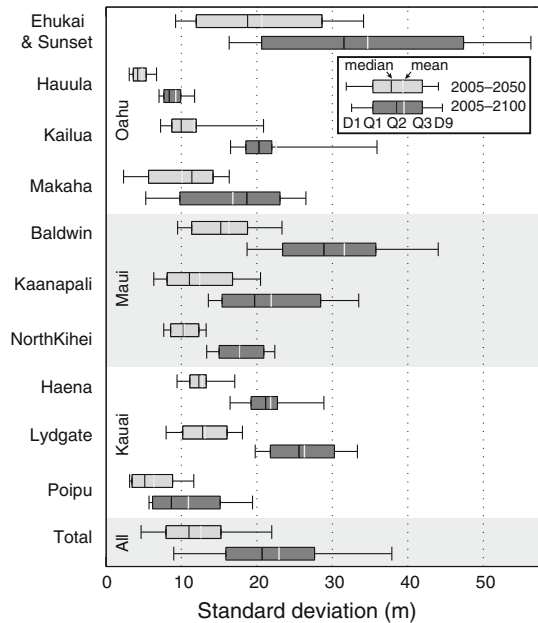
^a The projected net change from *additional SLR only* is a function of the difference between predicted and historical sea level, and nearshore slope (third term on right-hand side of Eq. 4). Of these input arguments, only the nearshore slope varies both within and among study regions. However, when only one profile location is present within a study region, all transects depend on the same nearshore slope; thus, the range of individual projections is zero, but the standard deviation of the mean is the nonzero standard deviation of the individual transect. This is consistent with areas of nonzero range, where individual standard deviations are used to calculate the standard deviation of the mean

Table 2 Mean shoreline change rates (\pm std) for historical, 2050, 2100 at each study site, and percent of retreating shorelines at each study site

Island	Region	Year	Average rate (m/year)	Range of rates (m/year)	Percent retreating
Oahu	Ehukai and Sunset	Historical	-0.08 ± 0.07	-0.69 to 0.68	65
		2050	-0.26 ± 0.07	-0.86 to 0.50	81
		2100	-0.40 ± 0.08	-1.01 to 0.34	95
	Hauula	Historical	-0.11 ± 0.00	-0.26 to 0.01	97
		2050	-0.25 ± 0.01	-0.39 to -0.13	100
		2100	-0.36 ± 0.01	-0.51 to -0.24	100
	Kailua	Historical	0.32 ± 0.03	-0.21 to 0.66	13
		2050	0.06 ± 0.05	-0.43 to 0.38	35
		2100	-0.15 ± 0.10	-0.61 to 0.20	66
	Makaha	Historical	-0.09 ± 0.02	-0.26 to 0.05	94
		2050	-0.19 ± 0.02	-0.36 to -0.05	100
		2100	-0.28 ± 0.03	-0.45 to -0.14	100
Maui	Baldwin	Historical	-0.12 ± 0.03	-1.87 to 0.81	57
		2050	-0.32 ± 0.02	-1.99 to 0.68	77
		2100	-0.49 ± 0.06	-2.09 to 0.58	80
	Kaanapali	Historical	-0.10 ± 0.03	-0.62 to 0.24	66
		2050	-0.30 ± 0.02	-0.84 to 0.12	84
		2100	-0.46 ± 0.04	-1.03 to 0.03	92
	North Kihei	Historical	-0.15 ± 0.03	-0.28 to -0.01	100
		2050	-0.30 ± 0.04	-0.41 to -0.14	100
		2100	-0.42 ± 0.06	-0.53 to -0.24	100
Kauai	Haena	Historical	-0.41 ± 0.01	-0.57 to -0.26	100
		2050	-0.55 ± 0.02	-0.69 to 0.68	100
		2100	-0.67 ± 0.02	-0.86 to 0.50	100
	Lydgate	Historical	-0.11 ± 0.01	-1.01 to 0.34	77
		2050	-0.45 ± 0.02	-0.26 to 0.01	100
		2100	-0.74 ± 0.11	-0.39 to -0.13	100
	Poipu	Historical	-0.19 ± 0.02	-0.51 to -0.24	98
		2050	-0.26 ± 0.02	-0.21 to 0.66	100
		2100	-0.32 ± 0.03	-0.43 to 0.38	100
All	Total	Historical	-0.05 ± 0.01	-1.87 to 0.81	67
		2050	-0.25 ± 0.01	-1.99 to 0.68	81
		2100	-0.42 ± 0.01	-2.09 to 0.58	90
	Total (excluding Kailua)	Historical	-0.13 ± 0.01	-1.87 to 0.81	79
		2050	-0.32 ± 0.01	-1.99 to 0.68	92
		2100	-0.48 ± 0.01	-2.09 to 0.58	96

change. Results, excluding Kailua, indicate that the average amount of shoreline recession roughly doubles by 2050 with increased SLR, compared to historic extrapolation alone. By 2100, accelerated SLR results in nearly 2.5 times the amount of shoreline recession based on historic extrapolation alone.

Fig. 12 Distributions of the standard deviation for each projected shoreline show that areas with large seasonal fluctuations (e.g., Ehukai and Sunset), large errors in profile slope (e.g., Lydgate), and short time series of historical data (e.g., Baldwin) have less precise projections



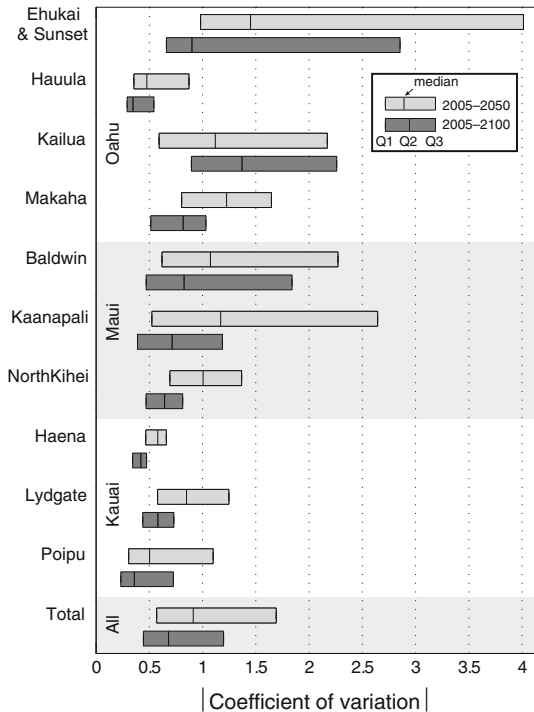
The standard deviations (stds) for the pdfs of net shoreline change vary between sites (Fig. 12) and range from 1.9 to 53.4 m in 2050 and 4.8 to 96.0 m in 2100. The median standard deviation over all locations is 11.0 m in 2050 and 20.7 m in 2100. We use the coefficient of variation (CV) to compare the ratios of the standard deviation (dispersion) to the mean (magnitude) (Fig. 13). The absolute value is appropriate because we are more interested in the ratio of the dispersion to the mean rather than whether the mean is negative (landward) or positive (seaward). Areas with high seasonal fluctuations that likely mask any underlying trend such as Ehukai and Sunset give larger CV values, whereas areas such as Hauula, where erosive trends are substantial and data errors are relatively small, produce smaller CV values.

4 Discussion

4.1 Sources of uncertainty

In the extrapolation of historical trends, areas with shorter time series, such as Baldwin and Kailua, have greater uncertainty in the long-term rate. Also, since shoreline aspect is related to wave climate, large seasonal fluctuations cause high uncertainty in historical shoreline models along north- and west-facing shorelines such as Sunset and Ehukai, Baldwin, and Kaanapali (refer to Fig. 3d). Alternative historical shoreline change models may improve predictions. Methods that include data at neighboring transects (instead of treating each transect independently), such as basis function methods (Frazer et al. 2009; Anderson and Frazer 2014) and regularization methods (Anderson et al. 2014), have been shown to improve long-term shoreline change modeling while slightly reducing the uncertainty in predictions.

Fig. 13 Box plots of CV values for each study area are displayed to compare the ratio of dispersion to magnitude. Areas such as Ehukai and Sunset have large CV values where noisy shorelines, as a result of large Pacific NW swells, create high uncertainty compared to relatively small predicted net change (any trends are likely masked by the noise in the data). Substantial trends in comparison with relatively *small data errors* generate smaller CV values. The mean of CV values is not shown in the box plot because it is not well behaved due to outlying values



In the R-DA model, uncertainty in the nearshore profile slope and SLR projections affect projected shorelines. Since shoreline response to relative SLR due to vertical land motion is accounted for in the historical trend, the uncertainty in the IPCC SLR projection is the same for all study sites. Uncertainty in the nearshore slope, however, does vary significantly between sites. At Lydgate, mid-Kaanapali, and the southern portion of Kailua, a shallow sand–reef intersection determines the seaward extent of the active profile. This, in combination with fluctuations in the beach toe position due to seasonal fluctuations at Kaanapali and Kailua, and tradewind fluctuations at Lydgate, causes high variability in the calculated nearshore slope. Thus, locations with both shallow reef platforms and unstable toe positions have larger uncertainty.

This study included the simplifying assumption that the profile shape of a beach adjacent to a reef platform would remain constant. It is likely, however, that changes in wave energy that reach the beach will alter the slope of the profile. More study is needed to see how beach profiles that terminate on reef platforms respond to sea level rise. Finally, it is prudent to keep in mind that in addition to the sources of uncertainty in model inputs discussed above, there is additional uncertainty in using the R-DA model in general, and uncertainty in neglecting changes in sediment transport patterns as a result of SLR and other climate-change-related aspects.

4.2 Assessment of the IPCC SLR scenario

The IPCC AR5 RCP 8.5 scenario shows the largest acceleration in SLR rate during the middle of the present century. In most areas (~80%), projected net shoreline change

(Fig. 10) for 2050 hovers between 1–24 m of landward migration, excluding the Kailua study area (discussed below). As a point of reference, most historical shoreline data errors range between 7–10 m. By 2100, on the other hand, projected net change increases to roughly 4–60 m of recession. It is important to keep in mind that these results do not include changes in sediment transport patterns due to changes in hydrodynamics resulting from increased water levels interacting with the fringing reef complex. Such changes are likely to reshape the equilibrium beach profile and lead to departures from the historical trends that are an important simplifying assumption of this model. Understanding of how these processes will affect future shorelines can be improved through a combination of hydrodynamical modeling and field monitoring at key representative beach sites.

4.3 Accretion at the reef-fringed pocket beach of Kailua, Oahu

The Kailua area was selected for its anomalously steady accretion over the last seven decades (Hwang 1981; Sea Engineering 1988; Norcross et al. 2003a). We find that Kailua Beach will continue accreting up to 2050 (Fig. 11), after which most of the beach will turn to an erosive state as SLR dominates, as indicated by the shoreline change rates estimated for 2100. However, the net migration projected for 2100 is predominantly positive (seaward of current shoreline; Figs. 8, 10) because, despite its erosive future behavior, it is not expected to erode past present locations by that time.

Since Kailua bay is bounded by basaltic headlands and there is a lack of modern sediment production (Harney et al. 2000), it is speculated that the sand-filled paleochannel that bisects the fringing reef in the middle of the bay acts as a conduit, supplying the beach with sediment from offshore. An example of a sand-filled paleochannel is shown in Fig. 3b. Since sand-filled channels such as this may often be the only offshore sand source for otherwise reef-fronted beaches, the effects of heightened sea level on sediment movement through channels warrant more research.

4.4 Spatial variation and limitations of linear extrapolation

The range of migration values (width of the boxes in Fig. 10) increases with time in all study areas. Extrapolating the historical shoreline change model into the future inherently assumes that sediment gain or loss rate is constant in time. Therefore, if a portion of a beach has historically lost sediment, but another portion of the same beach is, for some reason, gaining sediment, then over time, the two beach positions will continue to grow farther apart in the cross-shore direction. The continually diverging behavior is unrealistic over time. Yates et al. (2011) used expert knowledge to determine sections of the shoreline in which the alongshore average of the predicted shoreline could be used to represent the defined section. Others have taken a more objective approach, using an information criterion (e.g., Akaike, Schwartz) with alongshore basis functions (Frazer et al. 2009; Anderson and Frazer, 2014) or regularization (Anderson et al. 2014) to reduce the high-frequency fluctuations in rates and projections alongshore. The latter methods reduce unrealistic extremes at high spatial frequencies, while allowing long-wavelength variations in shoreline behavior. However, both methods rely on a time-linear sediment flux model, which will inevitably result in amplification of the alongshore variations over time (Anderson and Frazer 2014). So, while the magnitudes of rates are adjusted over time to reflect an increase in SLR, the range of the rates within an area will remain fairly consistent over time (Fig. 11). Conversely, because the sediment gain or loss rate at particular transects is

kept constant over time, the alongshore gradients in net migration must increase with time, depending on the historical shoreline change model employed (Fig. 10).

4.5 Sediment transport and SLR

In models based on the south Molokai, Hawaii coast, Grady et al. (2013) found that future SLR and climate-related reef degradation result in differing amounts of wave energy flux and thus alongshore sediment transport, over reefs of differing width. This indicates that reefs of varying width will experience alongshore changes in shoreline erosion and accretion under SLR. But how will increased SLR affect the highly variable geomorphology of Hawaiian beaches; will reef-fronted beaches (historically not exposed to high wave energy) experience enhanced recession compared to beaches adjacent to sand-filled paleochannels (historically exposed to high wave energy)? Results of hydrodynamic modeling for Molokai, Hawaii (Storlazzi et al. 2011) suggest that a 0.5–1.0-m SLR would increase coastal erosion and other physical processes (e.g., sediment re-suspension, mixing, and circulation). Climate-induced coral degradation may also increase wave energy reaching reef-fronted beaches as dissipation over the fringing reef is reduced (Sheppard et al. 2005). Thus, it is likely that increased water level over reef flats, in conjunction with potential reef degradation in Hawaii, will allow more wave energy to mobilize beach sand. Sand deposited beyond the outer reef edge during storm or high-swell events is subsequently prevented from returning to the beach by steep drop-offs at the outer reef edge. As noted above, Hawaii beaches generally lack any terrigenous sediment source and are composed of mainly ancient marine sediment grains, suggesting that modern sediment production does not sustain beaches, and therefore cannot be expected to mitigate the effects of SLR. Thus, it is likely that future SLR will result in a net loss of beach sand and exacerbate coastal erosion of Hawaiian reef-fronted beaches. The results of this study may then underestimate future recession.

Portions of north- and west-facing shores with deeper, more elongated, more irregular reefs may not experience as much erosion as other areas because the relative change in depth over reefs will be less. In their shoreline change analysis of the east coast of Florida, Houston and Dean (2014) find that an additional sediment source is required to account for chronic shoreline advance. They attribute onshore sediment transport from beyond the DoC as the source, probably as a result of episodic storms. Similarly, it is possible that the few Hawaii beaches fronted by paleochannels and/or deep reefs may gain sediment from offshore, thus buffering potentially erosive effects of SLR. Previous historical shoreline analysis (Fletcher et al. 2013) did not indicate less erosion of beaches fronted by deeper reefs, but such shorelines are typically associated with increased seasonal fluctuation that can mask the underlying long-term trend. The potential landward movement of offshore sediment, at both beaches adjacent to paleochannels and reef-fronted beaches, requires further study.

5 Conclusions

We analyzed net shoreline change at ten study sites across Hawaii for the years 2050 and 2100 under the IPCC AR5 RCP 8.5 SLR scenario. By combining historical extrapolation and the R-DA model for shoreline response to SLR, we produced probabilistic estimates of coastal erosion hazard areas. Erosion hazard zones can then be overlaid on GIS layers of

interest, and statistical analyses of coastal exposure to projected erosion hazards and shoreline change rates performed. These probabilistic model results provide a long-range management tool by identifying coastal lands and resources that are exposed to erosion under rising sea levels.

Approximately 92 and 96 % of the shorelines in the study area (excluding Kailua) are expected to be retreating by 2050 and 2100, respectively. Due to increasing SLR, the average shoreline recession by 2050 is nearly twice the historical extrapolation, and by 2100 it is nearly 2.5 times the historical extrapolation. Most projections (~80 %) range between 1–24 m of landward movement by 2050 and 4–60 m by 2100, except for Kailua. The average net shoreline change projected for Kailua is 7.1 ± 3.2 m of shore advance by 2050, reducing to 4.9 ± 6.8 m by 2100. Compared with net shoreline change projections based on historical extrapolation alone, projections that include excess SLR showed an average of about 6 m of additional shoreline recession by 2050 (relative to 2005) and 20 m by 2100 over all beaches in the study.

The average standard deviation for individual projections at all study sites is roughly 13 m for 2050 and 23 m for 2100. North- and west-facing beaches show increased uncertainty in erosion hazard projections as a result of Pacific NW swells in winter. The Baldwin area, in which the historical data series was truncated to reduce the effects of sand mining, also has larger uncertainty. Areas fronted by shallow reef flats that are susceptible to fluctuations in beach toe position due to NW swells or tradewinds have high inherent uncertainty due to the instability of the nearshore slope.

Increased water levels over fringing reefs and potential climate-related reef degradation will likely cause an increase in wave energy reaching the beach, which will mobilize more sediment. Sediment lost to offshore deposits beyond the outer reef drop-off will be isolated from the active beach system causing increased coastal erosion, especially given the lack of modern beach sediment production in Hawaii. Beaches fronted by deep or minimal reef cover may be able to keep pace with SLR. More studies of potential offshore sediment sources either directly over the DoC or through deep, sand-filled paleochannels are warranted.

Acknowledgments We thank Sam Lemmo of the Hawaii Department of Land and Natural Resources (DLNR) Office of Conservation and Coastal Lands (OCCL) for help in determining the needs of Hawaii's planning community. Funding for this study was provided by the Hawaii DLNR and the Department of Interior Pacific Islands Climate Science Center. This study was funded by the Hawaii Department of Land and Natural Resources and the Department of Interior Pacific Islands Climate Science Center.

Conflict of interest The authors declare that they have no conflict of interest.

References

- Anderson TR, Frazer LN (2014) Toward parsimony in shoreline change prediction (III): B-splines and noise handling. *J Coast Res* 30(4):729–742
- Anderson TR, Frazer LN, Fletcher CH (2014) Long-term shoreline change at Kailua, Hawaii using regularized single transect. *J Coast Res*. doi:10.2112/jcoastres-d-13-00202.1
- Aucan JP (2006) Directional wave climatology for the Hawaiian Islands from buoy data and the influence of ENSO on extreme wave events from wave model hindcast. In: Proceedings of the 9th International Workshop on Wave Hindcasting and Forecasting (Victoria, British Columbia), JCOMM Technical Report 34/WMO-TD, 1368
- Aucan JP, Hoeke R, Merrifield M (2012) Wave-driven sea level anomalies at the Midway tide gauge as an index of North Pacific storminess over the past 60 years. *Geophys Res Lett* 39(17):L17603. doi:10.1029/2012GL052993
- Bauer BO, Allen JR (1995) Beach steps: an evolutionary perspective. *Mar Geol* 123(3–4):143–166

- Bayley GV, Hammersley JM (1946) The “effective” number of independent observations in an autocorrelated time series. *Suppl J R Stat Soc* 8(2):184–197
- Bochicchio C, Fletcher CH, Dyer M, Smith T (2009) Reef-top sediment bodies: Windward Oahu, Hawaii. *Pac Sci* 63(1):61–82
- Bodge KR, Sullivan S (1999) Hawaii pilot beach restoration project: coastal engineering investigation. State of Hawaii Department of Land and Natural Resources, Honolulu, pp 38–40
- Bruun P (1962) Sea-level rise as a cause of shoreline erosion. *J Waterw Harb Div Am Soc Civ Eng* 88:117–130
- Bruun P (1988) The Bruun Rule of erosion by sea level rise: a discussion on large-scale and two- and three-dimensional usages. *J Coast Res* 4(4):627–648
- Caccamise DJ, Merrifield MA, Bevis M, Foster J, Firing Y, Schenewerk M, Taylor F, Thomas D (2005) Sea level rise at Honolulu and Hilo, Hawaii: GPS estimates of differential land motion. *Geophys Res Lett* 32:L03607. doi:10.1029/2004GL021380
- Calhoun RS, Fletcher CH (1996) Late Holocene coastal plain stratigraphy and sea level history at Hanalei, Kauai, Hawaii Islands. *Quat Res* 45(1):47–58
- Cazenave A, Le Cozannet G (2013) Sea level rise and its coastal impacts. *Earth Future* 2(2):15–34. doi:10.1002/2013EF000188
- Church JA, White NJ (2011) Sea-level rise from the late 19th to the early 21st century. *Surv Geophys* 32(4–5):585–602
- Church JA, Clark PU, Cazenave A, Gregory JM, Jevrejeva S, Levermann A, Merrifield MA, Milne GA, Nerem RS, Nunn PD, Payne AJ, Pfeffer WT, Stammer D, Unnikrishnan AS (2013) Sea level change. In: Stocker TF, Qin D, Plattner G-K, Tignor M, Allen SK, Boschung J, Nauels A, Xia Y, Bex V, Midgley PM (eds) *Climate change 2013: The physical science basis. Contribution of working group I to the fifth assessment report of the Intergovernmental Panel on Climate Change*. Cambridge University Press, Cambridge and New York
- Conger C (2005) Identification and characterization of sand deposit distribution on the fringing reefs of Oahu, Hawaii. Thesis, University of Hawaii at Manoa
- Cooper JAG, Pilkey OH (2004) Sea-level rise and shoreline retreat: time to abandon the Bruun Rule. *Glob Planet Change* 43:157–171
- Cowell PJ, Kench PS (2000) The morphological response of atoll islands to sea-level rise. Part 1: Modifications to the shoreface translation model. *J Coast Res Special Issue* 34, (ICS 2000, New Zealand), pp 633–644
- Cowell PJ, Roy PS, Jones RA (1995) Simulation of large-scale coastal change using a morphological behaviour model. *Mar Geol* 126(1–4):45–61
- Curtiss JH (1941) On the distribution of the quotient of two change variables. *Ann Math Stat* 12(4):409–421
- Daill HJ, Merrifield MA, Bevis M (2000) Steep beach morphology changes due to energetic wave forcing. *Mar Geol* 162(2–4):443–458
- Davidson-Arnott R (2005) Conceptual model of the effects of sea level rise on sandy coasts. *J Coast Res* 21(6):1166–1172
- Davison AC (2003) *Statistical models*. Cambridge University Press, Cambridge, p 726
- Dean RG (1991) Equilibrium beach profiles: characteristics and applications. *J Coast Res* 7(1):53–84
- Dean RG, Maurmeyer EM (1983) Models for beach profile response. In: Komar PD (ed) *CRC handbook of coastal processes and erosion*. CRC Press, Boca Raton, pp 151–165
- Douglas BC, Crowell M (2000) Long-term shoreline position prediction and error propagation. *J Coast Res* 16(1):145–152
- EUROSION (2004) Living with coastal erosion in Europe: sediment and space for sustainability. Part III—Methodology for assessing regional indicators
- Everts CH (1985) Sea level rise effects. *J Waterw Port Coast Ocean Eng* 111(6):985–999
- Fenneman MM (1902) Development of the profile of equilibrium of the subaqueous shore terrace. *J Geol* 10(1):1–32
- Fitzgerald DM, Fenster MS, Argow BA, Buynevich IV (2008) Coastal impacts due to sea-level rise. *Annu Rev Earth Planet Sci* 36:601–647
- Fletcher CH, Jones AT (1996) Sea-level highstand recorded in Holocene shoreline deposits on Oahu, Hawaii. *J Sediment Res* 66(3):632–641
- Fletcher CH, Rooney J, Barbee M, Lim S-C, Richmond B (2003) Mapping shoreline change using digital orthophotogrammetry on Maui, Hawaii. *J Coast Res SI*(38):106–124
- Fletcher CH, Murray-Wallace CV, Glenn CR, Sherman CE, Popp B, Hessler A (2005) Age and origin of late Quaternary eolianite, Kaiehu Point (Moomomi), Molokai, Hawaii. *J Coast Res SI*(42):97–112

- Fletcher CH, Bochicchio C, Conger CL, Engels MS, Feirstein EJ, Grossman EE, Grigg R, Harney JN, Rooney JJB, Sherman CE, Vitousek S, Rubin K, Murray-Wallace CV (2008) Geology of Hawaii reefs. In: Riegl BM, Dodge RE (eds) Coral reefs of the USA. Springer, New York, pp 435–488
- Fletcher CH, Romine BM, Genz AS, Barbee MM, Dyer M, Anderson TR, Lim SC, Vitousek S, Bochicchio C, Richmond BM (2013) National assessment of shoreline change: historical shoreline change in the Hawaiian Islands. U.S. Geological Survey Open-File Report 2011–1051
- Frazer LN, Genz AS, Fletcher CH (2009) Toward parsimony in shoreline change prediction (I): methods. *J Coast Res* 25(2):366–379
- Gibb JG (1995) Assessment of Coastal Hazard Zones for Northern Poverty Bay and Wainui Beach, Gisborne District. Report for the Gisborne District Council
- Gibbs AE, Richmond BM, Fletcher CH, Hillman KP (2001) Hawaii Beach Monitoring Program: Beach profile data. U.S. Geological Survey Open-File Report 01-308
- Grady AE, Moore LJ, Storlazzi CD, Elias E, Reidenbach MA (2013) The influence of sea level rise and changes in fringing reef morphology on gradients in alongshore sediment transport. *Geophys Res Lett* 40(12):3096–3101
- Grossman EE, Fletcher CH (1998) Sea level higher than present 3500 years ago on the northern main Hawaiian Islands. *Geology* 26(4):363–366
- Grossman EE, Fletcher CH (2004) Holocene reef development where wave energy reduces accommodation space, Kailua Bay, windward Oahu, Hawaii, USA. *J Sediment Res* 74(1):49–63
- Gutierrez BT, Plant NG, Thieler ER (2011) A Bayesian network to predict coastal vulnerability to sea level rise. *J Geophys Res* 116(F2):F02009. doi:10.1029/2010JF001891
- Hallermeier RJ (1981) A profile zonation for seasonal sand beaches from wave climate. *Coast Eng* 4:253–277
- Hands EG (1979) Changes in rates of shore retreat, Lake Michigan, 1967–1976. Coastal Engineering Research Center Technical Memorandum No. 79-4
- Hands EB (1980) Prediction of shore retreat and nearshore profile adjustments to rising water levels on the Great Lakes. Coastal Engineering Research Center Technical Memorandum No. 80-7
- Hands EB (1983) The Great Lakes as a test model for profile response to sea level changes. In: Komar PD (ed) Handbook of coastal processes and erosion. CRC Press, Boca Raton, pp 167–189
- Hanson H, Aarninkhof S, Capobianco M, Jimenez JA, Larson M, Nicholls RJ, Plant NG, Southgate HN, Steetzel HJ, Stive MJF, de Vriend HJ (2003) Modelling of coastal evolution on yearly to decadal time scales. *J Coast Res* 19(4):790–811
- Hapke CJ, Himmelstoss EA, Kratzman MG, List JH, Thieler ER (2010) National assessment of shoreline change: Historical shoreline changes along the New England and Mid-Atlantic coasts. U.S. Geological Survey Open-File Report 2010-1118
- Harney JN, Grossman EE, Richmond BM, Fletcher CH (2000) Age and composition of carbonate shoreface sediments, Kailua Bay, Oahu, Hawaii. *Coral Reefs* 19(2):141–154
- Helm V, Humbert A, Miller H (2014) Elevation and elevation change of Greenland and Antarctica derived from CryoSat-2. *Cryosphere Discuss* 8(2):1673–1721. doi:10.5194/tcd-8-1673-2014
- Hemer MA, Fan Y, Mori N, Semedo A, Wang XL (2013) Projected changes in wave climate from a multi-model ensemble. *Nat Clim Change* 3:471–476. doi:10.1038/nclimate1791
- Houston JR, Dean RG (2014) Shoreline change on the East Coast of Florida. *J Coast Res* 30(4):647–660
- Hwang DJ (1981) Beach changes on Oahu as revealed by aerial photographs, Honolulu, Hawaii: University of Hawaii, Hawaii Institute of Geophysics, Technical Report HIG-81-3, pp 66–75
- Hwang DJ (2005) Hawaii Coastal Hazard Mitigation Guidebook, Honolulu, Hawaii: University of Hawaii Sea Grant College Program, Report UNIH-SEAGRANT-BA-03-01
- Joughin I, Smith BE, Medley B (2014) Marine ice sheet collapse potentially underway for the Thwaites Glacier Basin, West Antarctica. *Science* 344(6185):735–738
- Katsman CA, Sterl A, Beersma JJ, van den Brink HW, Church JA, Hazeleger W, Kopp RE, Kroon D, Kwadijk J, Lammersen R, Lowe J, Oppenheimer M, Plag H-P, Ridley J, von Storch H, Vaughan DG, Vellinga P, Vermeersen LLA, van de Wal RSW, Weisse R (2011) Exploring high-end scenarios for local sea level rise to develop flood protection strategies for a low-lying delta—the Netherlands as an example. *Clim Change* 109(3–4):617–645
- Komar PD (1998) Beach processes and sedimentation, 2nd edn. Prentice-Hall, Upper Saddle River
- Komar PD, McDougal WG, Marra JJ, Ruggiero P (1999) The rational analysis of setback distances: applications to the Oregon Coast. *Shore and Beach* 76(1):41–49
- Kopp RE, Horton RM, Little CM, Mitrovica JX, Oppenheimer M, Rasmussen DJ, Strauss BH, Tebaldi C (2014) Probabilistic 21st and 22nd century sea-level projections at a global network of tide-gauge sites. *Earth's Future* 2(8):383–406. doi:10.1002/2014EF000239

- List JH, Sallenger AH Jr, Hansen ME, Jaffe BE (1997) Accelerated relative sea-level rise and rapid coastal erosion: testing a causal relationship for the Louisiana barrier islands. *Mar Geol* 140(3–4):347–365
- Merrifield MA, Maltrud ME (2011) Regional sea level trends due to a Pacific trade wind intensification. *Geophys Res Lett* 38(21):L21605
- Mimura N, Nobuoka H (1995) Verification of the Bruun Rule for the estimate of shoreline retreat caused by sea-level rise. In: Dally ER, Zeidler RB (eds) *Coastal dynamics 95*. American Society of Civil Engineers, New York, pp 607–616
- Moberly RM, Chamberlain T (1964) *Hawaiian beach systems*. Honolulu, Hawaii: University of Hawaii, Institute of Geophysics, Final Report HIG-64-2
- Moore JG (1970) Relationship between subsidence and volcanic load, Hawaii. *Bull Volcanol* 34(2):562–576
- Muñoz-Pérez JJ, Tejedor L, Medina R (1999) Equilibrium beach profile model for reef-protected beaches. *J Coast Res* 15(4):950–957
- Norcross ZM, Fletcher CH, Merrifield M (2003a) Annual and interannual changes on a reef-fringed pocket beach: Kailua Bay, Hawaii. *Mar Geol* 190(3–4):553–580
- Norcross Z, Fletcher CH, Rooney JJR, Eversole D, Miller TL (2003b) Hawaiian beaches dominated by longshore transport. In: Davis RA, Howd P, Sallenger A (eds) *Proceedings of the international conference on coastal sediments 2003*, Clearwater, Florida, 18–23 May 2003
- Péquignet A-CN, Becker J, Merrifield MA (2014) Energy transfer between wind waves and low-frequency oscillations on a fringing reef, Ipan, Guam. *J Geophys Res Oceans* 119(10):6709–6724
- Perry CT, Kench PS, Smithers SG, Riegl B, Yamano H, O’Leary MJ (2011) Implications of reef ecosystem change for the stability and maintenance of coral reef islands. *Glob Change Biol* 17(12):3679–3696
- Pilkey OH, Cooper JAG (2004) Society and sea level rise. *Science* 303(5665):1781–1782
- Pilkey OH, Young RS, Riggs SR, Sam Smith AW, Wu H, Pilkey W (1993) The concept of shoreface profile of equilibrium: a critical review. *J Coast Res* 9(1):255–278
- Purdy E (1974) Karst-determined facies patterns in British Honduras: Holocene carbonate sedimentation model. *Am As Pet Geol Bull* 58(5):825–855
- Ranasinghe R, Stive MJF (2009) Rising seas and retreating coastlines. *Clim Change* 97:465–468. doi:10.1007/s10584-009-9593-3
- Ranasinghe R, Callaghan D, Stive MJF (2011) Estimating coastal recession due to sea level rise: beyond the Bruun rule. *Clim Change* 110(3–4):561–574
- Rignot E, Mouginot J, Morlighem M, Seroussi H, Scheuchi B (2014) Widespread rapid grounding line retreat of Pine Island, Thwaites, Smith, and Kohler glaciers, West Antarctica, from 1992 to 2011. *Geophys Res Lett* 41(10):3502–3509
- Romine BM, Fletcher CH (2013) A summary of historical shoreline changes on beaches of Kauai, Oahu, and Maui: Hawaii. *J Coast Res* 29(3):605–614
- Romine BM, Fletcher CH, Barbee MM, Anderson TR, Frazer LN (2013) Are beach erosion rates and sea level rise related in Hawaii? *Glob Planet Change* 108:149–157. doi:10.1016/j.gloplacha.2013.06.009
- Romine, BM, Fletcher CH, Frazer LN, Anderson TR. Antecedent geomorphology and shoreline change, northeast Oahu, Hawaii. *J Geophys Res Earth Surf* (in review)
- Rooney JJB, Fletcher CH (2005) Shoreline change and pacific climatic oscillations in Kihei, Maui, Hawaii. *J Coast Res* 21(3):535–547
- Rosati JD, Dean RG, Walton TL (2013) The modified Bruun Rule extended for landward transport. *Mar Geol* 340:71–78
- Schwartz ML (1967) The Bruun theory of sea-level rise as a cause of shore erosion. *J Geol* 75(1):76–92
- SCOR Working Group 89 (1991) The response of beaches to sea-level changes: a review of predictive models. *J Coast Res* 7(3):895–921
- Sea Engineering (1988) *Oahu Shoreline Study, Part 1, Data on Beach Changes*. Honolulu, Hawaii. Report for the City and County of Honolulu Department of Land Utilization
- Shand T, Shand R, Reinen-Hamill R, Carley J, Cox R (2013) A review of shoreline response models to changes in sea level. In: *Coasts and Ports 2013: 21st Australasian Coastal and Ocean Engineering conference and the 14th Australasian Port and Harbour conference* (Sydney, Australia), pp 676–684
- Sheppard C, Dixon D, Gourlay M, Sheppard A, Payet R (2005) Coral mortality increases wave energy reaching shores protected by reef flats: examples from the Seychelles. *Estuar Coast Shelf Sci* 64(2–3):223–234
- Stive MJF (2004) How important is global warming for coastal erosion? An editorial comment. *Clim Change* 64(1–2):27–39
- Stive MJF, Aarninkhof SGJ, Hamm L, Hanson H, Larson M, Wijnberg KM, Nicholls RJ, Capobianco M (2002) Variability of shore and shoreline evolution. *Coast Eng* 47(2):211–235
- Storlazzi CD, Elias E, Field ME, Presto MK (2011) Numerical modeling of the impact of sea-level rise on fringing coral reef hydrodynamics and sediment transport. *Coral Reefs* 30(1 Supplement):83–96

- Thieler ER, Pilkey OH Jr, Young RS, Bush DM, Chai F (2000) The use of mathematical models to predict beach behavior for US coastal engineering: a critical review. *J Coast Res* 16(1):48–70
- Vitousek S, Fletcher CH (2008) Maximum annually recurring wave heights in Hawaii. *Pac Sci* 62(4):541–553
- Wang XL, Feng Y, Swail VR (2014) Changes in global ocean wave heights as projected using multimodel CMIP5 simulations. *Geophys Res Lett* 41:1026–1034. doi:[10.1002/2013GL058650](https://doi.org/10.1002/2013GL058650)
- Yates ML, Le Cozannet G (2012) Brief communication “Evaluating European coastal evolution using Bayesian networks”. *Nat Hazards Earth Syst Sci* 12(4):1173–1177
- Yates ML, Le Cozannet G, Lenotre N (2011) Quantifying errors in long-term coastal erosion and inundation hazard assessments. In: *Proceedings of the 11th international coastal symposium (Szczecin, Poland)*, pp 260–264
- Zhang K, Douglas BC, Leatherman SP (2004) Global warming and coastal erosion. *Clim Change* 64(1–2):41–58